



HAL
open science

Low- water maps of the groundwater table in the central Amazon by satellite altimetry

J. Pfeffer, F. Seyler, Marie-Paule Bonnet, S. Calmant, Frédéric Frappart, F. Papa, R. C. D. Paiva, F. Satge, J. S. da Silva

► To cite this version:

J. Pfeffer, F. Seyler, Marie-Paule Bonnet, S. Calmant, Frédéric Frappart, et al.. Low- water maps of the groundwater table in the central Amazon by satellite altimetry. *Geophysical Research Letters*, 2014, 41 (6), pp.1981-1987. 10.1002/2013gl059134 . hal-01016593

HAL Id: hal-01016593

<https://hal.science/hal-01016593v1>

Submitted on 6 Apr 2021

HAL is a multi-disciplinary open access archive for the deposit and dissemination of scientific research documents, whether they are published or not. The documents may come from teaching and research institutions in France or abroad, or from public or private research centers.

L'archive ouverte pluridisciplinaire **HAL**, est destinée au dépôt et à la diffusion de documents scientifiques de niveau recherche, publiés ou non, émanant des établissements d'enseignement et de recherche français ou étrangers, des laboratoires publics ou privés.



RESEARCH LETTER

10.1002/2013GL059134

Key Points:

- Groundwater and surface waters coincide during low-water periods
- First groundwater maps in central Amazon by satellite altimetry
- Interannual memory effects are observed in the central Amazon groundwater system

Supporting Information:

- Readme
- Appendix S1
- Appendix S2
- Appendix S3
- Figure S1

Correspondence to:

J. Pfeffer,
julia.pfeffer@ens-lyon.fr

Citation:

Pfeffer, J., F. Seyler, M.-P. Bonnet, S. Calmant, F. Frappart, F. Papa, R. C. D. Paiva, F. Satgé, and J. S. D. Silva (2014), Low-water maps of the groundwater table in the central Amazon by satellite altimetry, *Geophys. Res. Lett.*, *41*, 1981–1987, doi:10.1002/2013GL059134.

Received 31 JAN 2014

Accepted 21 FEB 2014

Accepted article online 3 MAR 2014

Published online 24 MAR 2014

Low-water maps of the groundwater table in the central Amazon by satellite altimetry

Julia Pfeffer^{1,2}, Frédérique Seyler^{3,4}, Marie-Paule Bonnet^{1,4}, Stéphane Calmant^{4,5}, Frédéric Frappart^{1,5}, Fabrice Papa^{5,6}, Rodrigo C.D. Paiva^{7,8}, Frédéric Satgé¹, and Joecila Santos Da Silva^{4,9}

¹Université de Toulouse, IRD, GET, Toulouse, France, ²Laboratoire de Géologie de Lyon: Terre, Planètes, Environnement, Université de Lyon, Ecole Normale Supérieure de Lyon, CNRS UMR 5276, Villeurbanne, France, ³UMR 228 ESPACE-DEV (IRD, UAG, UM2, UR), Cayenne, French Guiana, France, ⁴International Joint Laboratory LMI-OCE, IRD/University of Brasilia, Brasilia, Brazil, ⁵Université de Toulouse, IRD, LEGOS, Toulouse, France, ⁶Indo-French Cell for Water Sciences, IISc-NIO-IITM-IRD Joint International Laboratory, IISc, Bangalore, India, ⁷Universidade Federal do Rio Grande do Sul, IPH, Porto Alegre, Brazil, ⁸Byrd Polar Research Center, Ohio State University, Columbus, Ohio, USA, ⁹Universidade do Estado do Amazonas, CESTU, Manaus, Brazil

Abstract Groundwater plays a fundamental role in rainforest environments, as it is connected with rivers, lakes, and wetlands, and helps to support wildlife habitat during dry periods. Groundwater reservoirs are however excessively difficult to monitor, especially in large and remote areas. Using concepts from groundwater-surface water interactions and ENVISAT altimetry data, we evaluated the topography of the groundwater table during low-water periods in the alluvial plain of the central Amazon. The water levels are monitored using an unprecedented coverage of 491 altimetric stations over surface waters in the central Amazon. The groundwater table maps interpolated at spatial resolutions ranging from 50 to 100 km are consistent with groundwater wells data. They provide evidence of significant spatiotemporal organization at regional scale: heterogeneous flow from the hillslope toward the main rivers is observed, as well as strong memory effects and contrasted hydrological behaviors between the North and the South of the Amazon.

1. Introduction

The central Amazon region harbors the world's largest rainforest and impacts global climate through water, carbon, and energy exchanges [e.g., Richey *et al.*, 2002]. Groundwater reserves are closely linked to this environment, as they store excess water during wet periods and sustain rivers, floodplains, wetlands, and related ecosystems during low-water periods [e.g., Lesack, 1993]. Groundwater contributes actively to the biogenic [e.g., Cullmann *et al.*, 2006] and geochemical fluxes [e.g., Neu *et al.*, 2011] across the Amazon and impedes water stress during dry periods through deep root uptake and hydraulic redistribution [e.g., Nepstad *et al.*, 1994; Oliveira *et al.*, 2005; Nepstad *et al.*, 2007; Vourlitis *et al.*, 2008].

Field investigations report a shallow groundwater table in the central Amazon, slowly converging toward valley bottoms, which generates seasonal seepage in lower floodplains [e.g., Lesack, 1995; Lesack and Melack, 1995; Cullmann *et al.*, 2006; Bonnet *et al.*, 2008] and accounts for most of river discharge in headwater catchments [e.g., Hodnett *et al.*, 1997a]. Strong memory effects are evidenced in groundwater systems, conveying climate anomalies for several years [e.g., Tomasella *et al.*, 2008]. Recent modeling approaches coupling surface and groundwater dynamics confirm the occurrence of these mechanisms through the Amazon River basin, even though the scarcity of data limits the quality of model predictions [e.g., Fan and Miguez-Macho, 2010; Miguez-Macho and Fan, 2012]. In particular, critical data evaluating the spatial and temporal variability of the groundwater table level is still lacking in the central Amazon.

Our study aims to provide the first regional maps of the groundwater table during low-water periods in the central Amazon. Our method relies on the use of satellite altimetry data and on the field investigation driven by Lesack [1993]; Lesack [1995]; Lesack and Melack [1995], Hodnett *et al.* [1997a, 1997b], and Cullmann *et al.* [2006], who established that during low-water periods the water stage in rivers, lakes, and floodplains coincides with the groundwater level (Figure 1). Surface water stages provide therefore direct information about the groundwater level during low-water periods, which can be monitored by satellite altimetry [e.g., Alsdorf *et al.*, 2001; Birkett *et al.*, 2002; Alsdorf *et al.*, 2007; Calmant *et al.*, 2008; Santos Da Silva *et al.*, 2012].

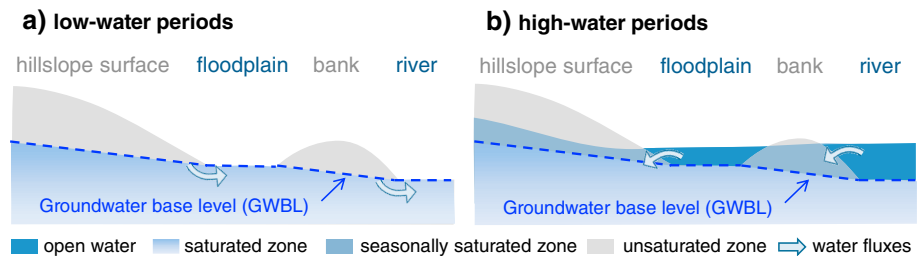


Figure 1. A simple scheme of groundwater and surface water exchanges in the central Amazon.

2. Materials and Methods

Our focus is to evaluate the topography of the groundwater table during low-water periods in the alluvial plain of the central Amazon region (Figure 2). Those lowlands (Figure 3a), largely inundated during high-water periods (Figure 2) [Hess *et al.*, 2003], are composed of alluvial deposits and of consolidated and unconsolidated sediments (Figure 2) [IBGE, 1990], with relatively homogeneous hydrogeological properties (see Gleeson *et al.* [2011] and Fan *et al.* [2013] for global maps of the groundwater properties). We defined the groundwater base level (GWBL) as the minimum water level at the closest river, lake, or floodplain connected to the alluvial aquifer (Figure 1). During low-water periods (Figure 1a), the residual bank storage received from floodwater infiltration becomes very low [Lesack, 1995]. Besides, the groundwater mounds formed from hillslope infiltration are small since the surface topography is very gentle (Figure 3a). The GWBL interpolated between the surfaces water stages (Figure 1, dashed line) provides thus a reasonable lower estimate of the groundwater table level during low-water periods in the central Amazon alluvial plain.

The ENVISAT altimetry data are used to estimate the elevations of surface water stages. Surface water heights are generated using the Virtual Altimetry Station software (VALS, 2011, version 1.06.07, available at <http://www.ore-hybam.org>) for 593 virtual stations located at the intersections between the satellite groundtrack and the rivers, lakes, and floodplains exceeding 100 m in width (Figure 2), using the same method as Santos *da Silva et al.* [2010, 2012]. Heights are converted into altitudes using the Earth Gravitational Model EGM2008 [Pavlis *et al.*, 2012]. Final altimetric time series span from late 2002 to mid-2009 with a temporal sampling of 35 days. The typical uncertainties of ENVISAT-derived water level time series, estimated by comparison with in situ gauges measurements located near the virtual stations, are less than 30 cm [Santos *Da Silva et al.*, 2010]. In addition, the ENVISAT data should be corrected for a 1.04 ± 0.21 m bias [Calmant *et al.*, 2013]. Subsequently, the elevations retrieved from the ENVISAT measurements can be considered to have a submetric uncertainty.

A selection process is then applied to the data. First, the virtual stations lying outside the alluvial plain are excluded from the data set. Second, the annual minima are selected in the time series of each virtual station, leading to at least six values at low water peaking between October and January each year. Third, the virtual stations, whose annual minima varied by less than 1 m during the 6 years of the study period were removed from the data set. Actually, during the 6 years of the study period, the central Amazon region experienced highly variable climatic conditions. We considered that if the ENVISAT water levels measurements did not vary significantly during this period, the low stages measurements were not reliable, presumably because that have been impacted by the emergence of islets, sand bars, land, or vegetation.

The GWBL maps are finally obtained using a natural neighbor interpolation [Sibson, 1981] between the 491 selected stations (on average, 6.11 stations per square degree), which provides smooth interpolated surfaces, tightly controlled by the original data points. Another interpolation technique was tested using additional a priori hydrological data, giving similar results at regional scale (supporting information Appendix S1). Slopes and flow directions are computed at the GWBL surface with the TopoToolbox developed by Schwanghart and Kuhn [2010].

3. Results

3.1. Spatial Organization of the Average GWBL

The average GWBL (Figure 3b) is computed over the 6 years of the study period. The average GWBL is a smoothed replica of the surface topography: it varies from 3 to 87 m along an east-west gradient. It is

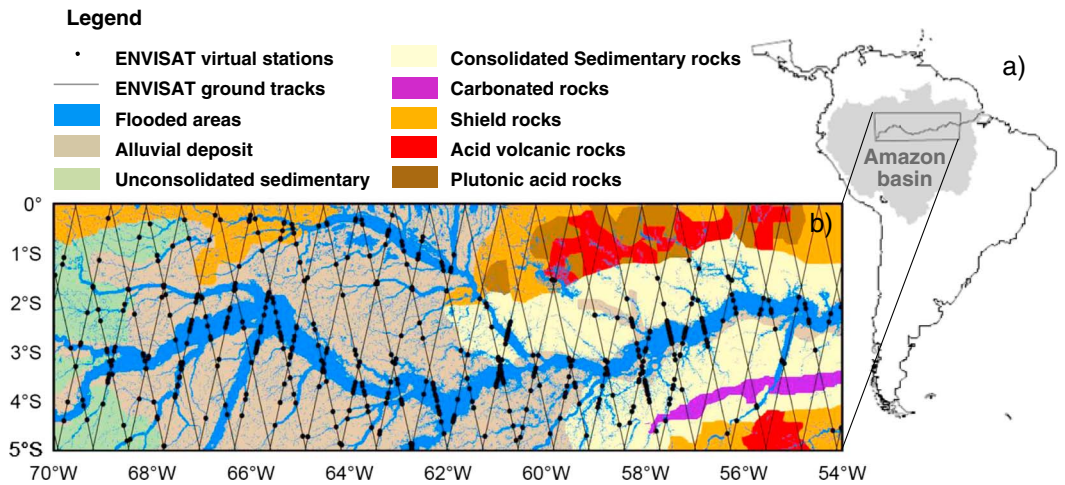


Figure 2. The central Amazon region. (a) Location of the study area in the Amazon basin. (b) Locations of all the ENVISAT virtual stations. Flooded areas [Hess et al., 2003] are in blue over the main geological units defined by the IBGE in 1990.

compared to groundwater table heights evaluated at 1540 wells, as the difference between the surface height derived from Shuttle Radar Topography Mission (SRTM) 3" Digital Elevation Model (DEM) (Figure 3a) [Farr et al., 2007] and the groundwater table depth compiled by Fan et al. [2013]. Large differences (from -70 up to 136 m) occur between the average GWBL and the groundwater table heights (see maps in supporting information Appendix S2), which can be attributed to mismatching scales and spatial sampling. This can be

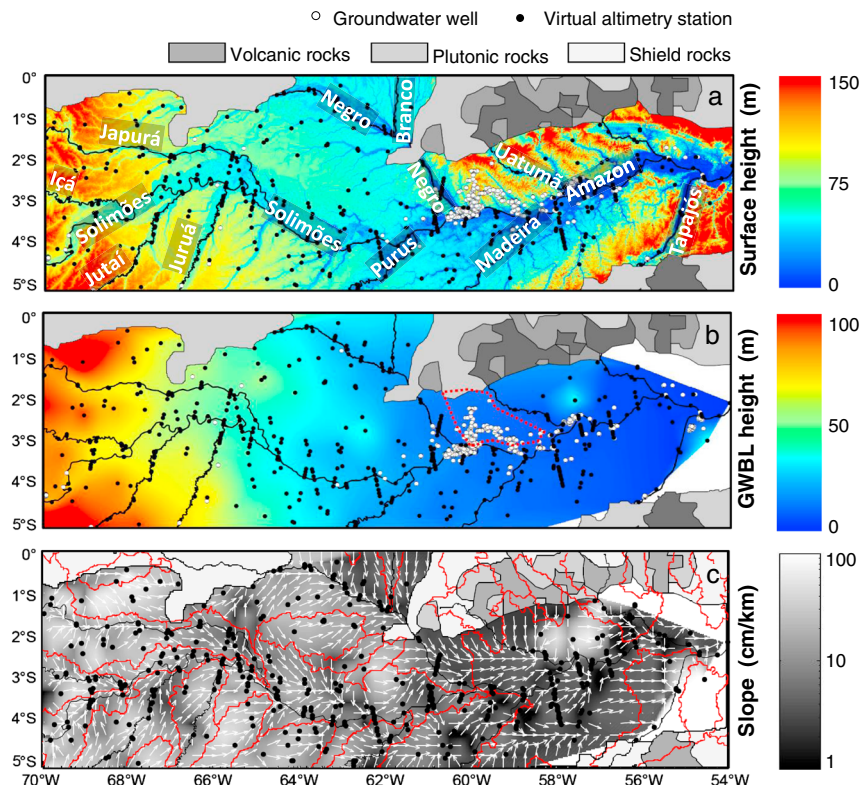


Figure 3. Topography, groundwater base level (GWBL), and flow directions in the central Amazon. (a) Surface topography derived from the SRTM 3" DEM referenced to EGM08. Main rivers are named in white. (b) Average GWBL over the 2003–2008 period. Zone 1 is delimited by a red hatched line. (c) Slopes (logarithmic color scale) and flow directions (white arrows) at the average GWBL. The boundaries of the Amazonian subbasins are in red.

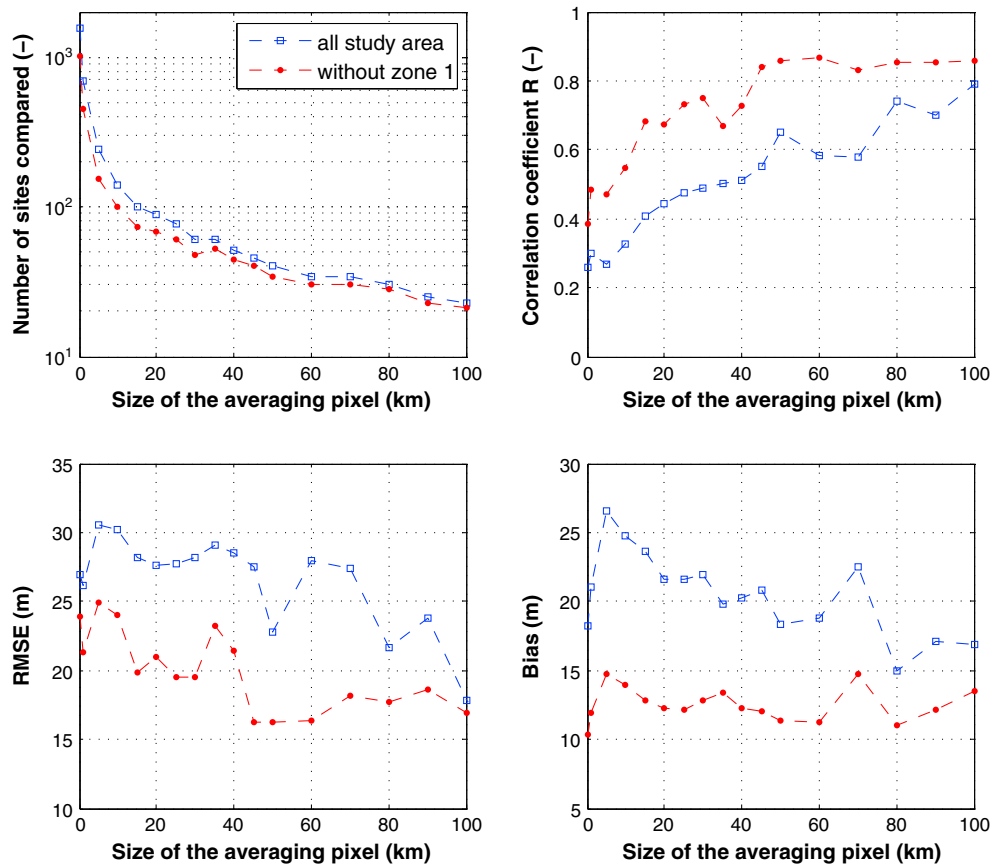


Figure 4. Comparison of the average GWBL with groundwater table elevations evaluated at 1540 wells averaged in growing pixels. Zone 1 is shown in Figure 3b. Please note that the upper left panel uses a logarithmic scale.

solved by averaging the data at spatial resolutions of several tens of kilometers. Higher correlation coefficients ($R > 0.6$, p -value $< 10^{-3}$) are indeed found when averaging groundwater table heights over regular grids with spatial resolutions ranging from 50 to 100 km (Figure 4; see scatter plots in supporting information Appendix S2). This correlation is further improved ($R \sim 0.86$, p -value $< 10^{-3}$) when excluding the wells located in zone 1 (Figure 4). In this region (Figure 3b), the value of the average GWBL relies solely on the interpolation between stations located on the Negro, the Uatumã, and the Amazon rivers and should thus be interpreted with caution. When excluding zone 1 and at 50 km resolution, the root mean square error (RMSE) is ~ 16 m between the average GWBL and the groundwater table heights. Besides, the use of the SRTM 3' DEM surface heights introduces errors in the groundwater height estimated at wells (RMSE = 13 m; see supporting information Appendix S2). Hence, it introduces noise in the comparison, which may account for a large part ($> 80\%$) of the differences and the RMSE observed between both groundwater estimates. It could however not explain the bias observed between both groundwater estimates. Indeed, at the point scale, the average GWBL is found to be ~ 11 m lower than the groundwater height estimated at wells (Figure 4). This may be because the average GWBL is evaluated during low-water periods, while the groundwater elevations estimated at wells do not relate to a specific time in the year. A bias of several meters can thus be expected over the whole study area. This effect should be uniform, or at least random, as it affects equally all virtual altimetry stations. Hence, it will have little effect on the estimate of gravity-driven groundwater flow (Figure 3c). In addition, due to the spatial sampling of the altimetry stations, groundwater mounds formed under topographic highs may not be detected at scales smaller than 50–100 km. This effect should however not affect regional features of the groundwater table topography. These results confirmed that the average GWBL is a lower estimate of the groundwater table height, valid at regional scale (larger than 50 km), during low-water periods, for relatively flat areas reasonably covered by virtual stations.

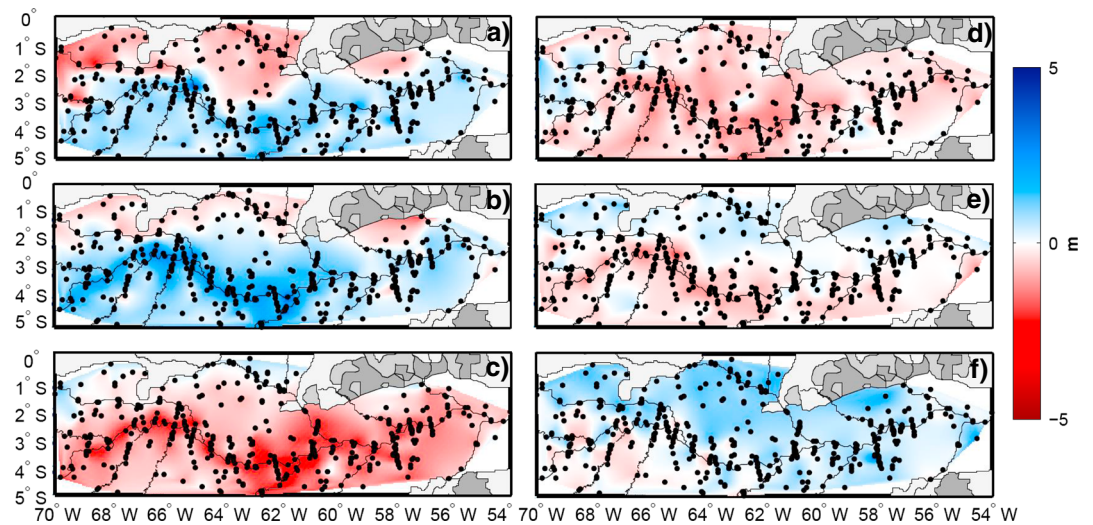


Figure 5. Deviation from the average groundwater base level in (a) 2003, (b) 2004, (c) 2005, (d) 2006, (e) 2007, and (f) 2008.

The average GWBL forms a continuous and connected drainage structure similar to the surface drainage network (Figure 3c). The gravitational flow computed at the GWBL surface is directed from the hillslope toward the main rivers and diverges at the main basin boundaries, except for the lower third of the Amazon region and for some of the tributary basins feeding the main tributaries of the Amazon (e.g., the Branco). The gravitational part of the GWBL flow is subjected to strong variations in amplitude proportional to the average GWBL slope ranging from 0.1 to 80 cm/km. The average GWBL flow is the highest at the west of the study area and decreases by 2 orders of magnitude in the lower third regions, which is consistent with the predominance of kinetic flow over gravitational flow in this area [Molinier *et al.*, 1996]. Along the main rivers, the average GWBL slope does not exceed a few centimeters per kilometer (supporting information Figure S1), in agreement with the surface water gradients evaluated by Birkett *et al.* [2002]. Besides, the slope values at the average GWBL are consistent with in situ observations of the groundwater table [e.g., Lesack, 1995; Cullmann *et al.*, 2006]. Similar patterns are observed each year, because the temporal variations in the GWBL are small (± 5 m; Figure 5) compared with its average spatial variations (75 m; Figure 3b).

3.2. Temporal Variations of the GWBL

From altimetry-derived water level time series, six annual minima are identified for each virtual station and used to evaluate the deviation from the average GWBL (i.e., the difference between a particular year and the 6 year average; Figure 4). The most striking feature is the reduction in the GWBL observed during the 2005 drought, which is particularly strong (4 m less than the average) along the Amazon and Solimões. In the northern regions, the GWBL is higher in 2005 than in the 6 year average. After the 2005 drought, the GWBL slowly rises from the north to the south. The GWBL recovers to its average value between 2007 and 2008, which suggested strong memory effects across the central Amazon. Further details concerning the temporal variations of the GWBL are given in Appendix S3 (supporting information).

4. Discussion

The spatial patterns evidenced in the average GWBL are consistent with in situ observations of the groundwater table averaged over a 50 km resolution grid. Field investigations [e.g., Lesack, 1993; Lesack, 1995; Lesack and Melack, 1995; Hodnett *et al.*, 1997a, 1997b; Cullmann *et al.*, 2006] also report that groundwater sustains the main rivers during low-water periods. These punctual observations are supported at basin scale by hydrological models [e.g., Miguez-Macho and Fan, 2012] and now at regional scale by altimeter-derived maps, showing GWBL flow convergence toward the main rivers (Figure 3c). For some tributaries, the surface basin boundaries are crossed by the GWBL flow. This can largely be attributed to the spatial sampling of the altimetry stations, which is insufficient to fully recover local-scale hydrological features. The predominance of kinetic flow over gravitational flow in the lower third of the Amazon region [Molinier *et al.*, 1996] should also

be considered, as well as potential interbasin groundwater flow [e.g., *Généreux and Jordan, 2006; Schaller and Fan, 2009*], which could be due to relatively recent fluvial capture in the Amazon basin [*Almeida-Filho and Miranda, 2007; Rossetti and Valeriano, 2007*].

Time-variable GWBL maps are consistent with the hydroclimatology of the Amazon. They illustrate the sensitivity of the groundwater table to extreme climatic events. A major drought, related to an anomalous northward position of Inter Tropical Convergence Zone, struck the Amazon in 2005 [e.g., *Marengo et al., 2008a; Zeng et al., 2008*]. Surface waters were strongly impacted along the Amazon mainstem [e.g., *Tomasella et al., 2011*], as well as in the southern and western regions of the Amazon [e.g., *Frappart et al., 2012*], while wet conditions prevailed in the northeastern Amazon [e.g., *Marengo et al., 2008b*]. Similarly, the groundwater table decreased by several meters during the 2005 drought, especially along the mainstem and in southern Amazon, while it rose in northeastern Amazon (Figure 4). This behavior is consistent with the minimum of the total water storage anomaly derived from Gravity Recovery And Climate Experiment data over the Amazon basin [*Frappart et al., 2013*]. In situ observations reveal strong memory effects in groundwater systems at local scale in Amazonia [*Tomasella et al., 2008*]. Annual GWBL maps (Figure 4) show that groundwater conveys the 2005 anomaly until 2008 for all the regions affected by the drought. This memory effect is doubled edged, as groundwater sustains stream flow and evaporation during dry periods, and may have an effect on rainfall deficit persistence [e.g., *Bierkens and van den Hurk, 2007*]. The dynamics of groundwater systems should thus be better considered when attempting to close the water balance in hydrological and atmospheric models for the Amazon basin.

5. Conclusions and Perspectives

Satellite radar altimetry offers a unique opportunity to monitor continental surface waters with full coverage and timely distribution across large river basins. We define 491 ENVISAT virtual stations in the central Amazon, leading to an unprecedented spatial coverage of the rivers, lakes, and floodplains stage variations at this scale. Assuming that the minima of the surface water stages coincide with the base level of the groundwater table, we provide the first maps of the GWBL across the central Amazon based on altimetry data. These were consistent with groundwater table elevations evaluated at 1540 wells, averaged over a 50 km resolution grid. Although local-scale features may not be adequately resolved, the GWBL maps provide valuable insight on the general hydrological behavior of the central Amazon:

1. During low-water periods, the groundwater table exhibits a strong spatial heterogeneity but forms a connected drainage structure mainly driven by the surface topography. The gravitational GWBL flow converges from the hillslope toward the main rivers and becomes negligible in the lower third of the central Amazon.
2. During the 2005 drought, the GWBL exhibits a contrasted behavior in the northern and southern parts of the Amazon. The GWBL rose in the north of 1.5°S when it decreased elsewhere in the central Amazon region. In 2006, the GWBL begins to rise again from the north to the south. It remains however lower than average for several years, which suggests strong memory effects at regional scale across the central Amazon.

The GWBL maps provide critical information about the spatial and temporal patterns of the groundwater table across the central Amazon region, which can be used to better represent groundwater in hydrological models and better understand hydrological processes at large scales. One should however keep in mind that the GWBL maps are only valid at regional scale, during low-water periods, in the alluvial plain of the central Amazon and for areas reasonably covered by virtual altimetry stations. Besides, the dense spatial sampling of the altimetric data set will benefit the calibration and validation of hydrological models, leading to better predictions of the impact of extreme climatic events on surface waters and to a better evaluation of the hydrological fluxes involved in the carbon cycle.

References

- Almeida-Filho, R., and F. P. Miranda (2007), Mega capture of the Rio Negro and formation of the Anavilhanas Archipelago, Central Amazônia, Brazil: Evidences in an SRTM digital elevation model, *Remote Sens. Environ.*, 110(3), 387–392, doi:10.1016/j.rse.2007.03.005.
- Alsdorf, D., C. Birkett, T. Dunne, J. Melack, and L. Hess (2001), Water level changes in a large Amazon lake measured with spaceborne radar interferometry and altimetry, *Geophys. Res. Lett.*, 28(14), 2671–2674.
- Alsdorf, D., E. Rodriguez, and D. P. Lettenmaier (2007), Measuring surface water from space, *Rev. Geophys.*, 45, RG2002, doi:10.1029/2006RG000197.
- Bierkens, M. F. P., and B. J. J. M. van den Hurk (2007), Groundwater convergence as a possible mechanism for multi-year persistence in rainfall, *Geophys. Res. Lett.*, 34, L02402, doi:10.1029/2006GL028396.

Acknowledgments

This research was supported by the project CARBAMA (CARBon biogeochemistry and atmospheric exchanges in the AMAZon river system) funded by the ANR (National Research Agency), the project MHYZPA (Modelisation de l'Hydrologie des zones d'inondation de la Plaine Centrale Amazonienne) funded by EC2CO (INSU/CNRS), the bilateral CNPq (Conselho Nacional de Desenvolvimento Científico e Tecnológico, Brazil), and the IRD (Institut de Recherche pour le Développement, France). The authors thank the Centre de Topographie des Océans et de l'Hydrosphère (CTOH) at Laboratoire d'Etudes en Géophysique et Océanographie Spatiales (LEGOS), France, for providing the ENVISAT RA-2 GDR data set. We are grateful to the ANA (Brazilian Water Agency) and the CPRM (Serviço geológico do Brasil) for providing support during the field trip and access to the hydrological data. We also thank Ying Fan Reinfelder and Tom Gleeson for their careful reviews. The data presented here, i.e., the minimum water heights measured at virtual altimetry stations and the low-water maps of the groundwater table, are freely available to the scientific community upon request to the authors. In a near future, these data will also be available via the CTOH (<http://ctoh.legos.obs-mip.fr>) and the LMI-OCE (<http://lmiocce.wordpress.com/>) websites.

The Editor thanks Ying Reinfelder and Tom Gleeson for their assistance in evaluating this paper.

- Birkett C., L. A. K. Mertes, T. Dunne, M. H. Costa, and M. J. Jasinski (2002), Surface water dynamics in the Amazon Basin: Application of satellite radar altimetry. *J. Geophys. Res.*, 107(D20), 8059, doi:10.1029/2001JD000609.
- Bonnet, M. P., et al. (2008), Floodplain hydrology in an Amazon floodplain lake (Lago Grande de Curuaí), *J. Hydrol.*, 349(1), 18–30.
- Calmant, S., F. Seyler, and J. F. Cretaux (2008), Monitoring continental surface waters by satellite altimetry, *Surv. Geophys.*, 29(4–5), 247–269.
- Calmant, S., J. S. da Silva, D. M. Moreira, F. Seyler, C. K. Shum, J. F. Cretaux, and G. Gabalda (2013), Detection of Envisat RA2/ICE-1 retracked radar altimetry bias over the Amazon basin rivers using GPS, *Adv. Space Res.*, 51(8), 1551–1564, doi:10.1016/j.asr.2012.07.033.
- Cullmann, J., W. J. Junk, G. Weber, and G. H. Schmitz (2006), The impact of seepage influx on cation content of a Central Amazonian floodplain lake, *J. Hydrol.*, 328(1), 297–305.
- Fan, Y., and G. Miguez-Macho (2010), Potential groundwater contribution to Amazon evapotranspiration, *Hydrol. Earth Syst. Sci.*, 14(10), 2039–2056.
- Fan, Y., H. Li, and G. Miguez-Macho (2013), Global patterns of groundwater table depth, *Science*, 339(6122), 940–943.
- Farr, T. G., et al. (2007), The Shuttle Radar Topography Mission, *Rev. Geophys.*, 45, RG2004, doi:10.1029/2005RG000183.
- Frappart, F., F. Papa, J. Santos da Silva, G. Ramillien, C. Prigent, F. Seyler, and S. Calmant (2012), Surface freshwater storage in the Amazon basin during the 2005 exceptional drought, *Environ. Res. Lett.*, 7(4), 044010, doi:10.1088/1748-9326/7/044010.
- Frappart, F., G. Ramillien, and J. Ronchail (2013), Changes in terrestrial water storage versus rainfall and discharges in the Amazon basin. *Int. J. Climatol.*, 33(14), 3029–3046, doi:10.1002/joc.3647.
- Généreux, D. P., and M. Jordan (2006), Interbasin groundwater flow and groundwater interaction with surface water in a lowland rainforest, Costa Rica: A review, *J. Hydrol.*, 320(3), 385–399.
- Gleeson, T., L. Smith, N. Moosdorf, J. Hartmann, H. H. Dürr, A. H. Manning, L. P. H. van Beek, and A. M. Jellinek (2011), Mapping permeability over the surface of the Earth, *Geophys. Res. Lett.*, 38, L02401, doi:10.1029/2010GL045565.
- Hess, L. L., J. M. Melack, E. M. Novo, C. C. Barbosa, and M. Gastil (2003), Dual-season mapping of wetland inundation and vegetation for the central Amazon basin, *Remote Sens. Environ.*, 87(4), 404–428.
- Hodnett, M. G., I. Vendrame, A. D. O. Marques Filho, M. D. Oyama, and J. Tomasella (1997a), Soil water storage and groundwater behaviour in a catenary sequence beneath forest in central Amazonia: I. Comparisons between plateau, slope and valley floor, *Hydrol. Earth Syst. Sci.*, 1(2), 265–277.
- Hodnett, M. G., I. Vendrame, A. D. O. Marques Filho, M. D. Oyama, and J. Tomasella (1997b), Soil water storage and groundwater behaviour in a catenary sequence beneath forest in central Amazonia II. Floodplain water table behaviour and implications for streamflow generation, *Hydrol. Earth Syst. Sci.*, 1(2), 279–290.
- IBGE (1990), Mapa Geologica do Brasil, Projeto RADAMBRASIL, atualizada 2006, Projeto Sistematização das Informações sobre Recursos Minerais, Projeção Albers, Datum SAD69, Escala 1:1000000. [Available at <http://mapas.ibge.gov.br/tematicos/geologia/>]
- Lesack, L. F. (1993), Water balance and hydrologic characteristics of a rain forest catchment in the central Amazon basin, *Water Resour. Res.*, 29(3), 759–773.
- Lesack, L. F. (1995), Seepage exchange in an Amazon floodplain lake, *Limnol. Oceanogr.*, 40(3), 598–609.
- Lesack, L. F., and J. M. Melack (1995), Flooding hydrology and mixture dynamics of lake water derived from multiple sources in an Amazon floodplain lake, *Water Resour. Res.*, 31(2), 329–345.
- Marengo, J. A., et al. (2008a), The drought of Amazonia in 2005, *J. Clim.*, 21(3), 495–516.
- Marengo, J. A., C. A. Nobre, J. Tomasella, M. F. Cardoso, and M. D. Oyama (2008b), Hydro-climatic and ecological behaviour of the drought of Amazonia in 2005, *Philos. T. R. Soc. B*, 363(1498), 1773–1778.
- Miguez-Macho, G., and Y. Fan (2012), The role of groundwater in the Amazon water cycle: 1. Influence on seasonal streamflow, flooding and wetlands, *J. Geophys. Res.*, 117, D15113, doi:10.1029/2012JD017539.
- Molinier, M., J. L. Guyot, E. De Oliveira, and V. Guimaraes (1996), Les régimes hydrologiques de l'Amazonie et de ses affluents, in *L'hydrologie tropicale: géosciences et outil pour le développement: mélanges à la mémoire de Jean Rodier*, pp. 209–222, Int. Ass. Hydrol. Sci. Publication, Wallingford, U. K.
- Nepstad, D. C., C. J. R. Carvalho, E. A. Davidson, P. H. Jipp, P. A. Lefebvre, G. H. Negreiros, E. D. da Silva, T. A. Stone, S. E. Trumbore, and S. Vieira (1994), The deep-soil link between water and carbon cycles of Amazonian forests and pastures, *Nature*, 372, 666–669.
- Nepstad, D. C., I. M. Tohver, D. Ray, P. Moutinho, and G. Cardinot (2007), Mortality of large trees and lianas following experimental drought in an Amazon forest, *Ecology*, 88(9), 2259–2269.
- Neu, V., C. Neill, and A. V. Krusche (2011), Gaseous and fluvial carbon export from an Amazon forest watershed, *Biogeochemistry*, 105(1–3), 133–147.
- Oliveira, R. S., T. E. Dawson, S. S. Burgess, and D. C. Nepstad (2005), Hydraulic redistribution in three Amazonian trees, *Oecologia*, 145(3), 354–363.
- Pavlis, N. K., S. A. Holmes, S. C. Kenyon, and J. K. Factor (2012), The development and evaluation of the Earth Gravitational Model 2008 (EGM2008), *J. Geophys. Res.*, 117, B04406, doi:10.1029/2011JB008916.
- Richey, J. E., J. M. Melack, A. K. Aufdenkampe, V. M. Ballester, and L. L. Hess (2002), Outgassing from Amazonian rivers and wetlands as a large tropical source of atmospheric CO₂, *Nature*, 416(6881), 617–620.
- Rossetti, D. F., and M. M. Valeriano (2007), Evolution of the lowest Amazon basin modeled from the integration of geological and SRTM topographic data, *Catena*, 70(2), 253–265, doi:10.1016/j.catena.2006.08.009.
- Santos da Silva, J., S. Calmant, F. Seyler, O. C. Rotunno Filho, G. Cochonneau, and W. J. Mansur (2010), Water levels in the Amazon basin derived from the ERS 2 and ENVISAT radar altimetry missions, *Remote Sens. Environ.*, 114(10), 2160–2181.
- Santos da Silva, J., S. Calmant, F. Seyler, H. Lee, and C. K. Shum (2012), Mapping of the extreme stage variations using ENVISAT altimetry in the Amazon basin rivers. *Int. J. Water*, 2(1), 14–26, <http://iwj.info/wp-content/uploads/2012/11/V2-N1-p2.pdf>.
- Schaller, M. F., and Y. Fan (2009), River basins as groundwater exporters and importers: Implications for water cycle and climate modeling, *J. Geophys. Res.*, 114, D04103, doi:10.1029/2008JD010636.
- Schwanghart, W., and H. J. Kuhn (2010), TopoToolbox: A set of Matlab functions for topographic analysis, *Environ. Modell. Software*, 25, 770–781, doi:10.1016/j.envsoft.2009.12.002.
- Sibson, R. (1981), A brief description of natural neighbour interpolation, in *Interpreting Multivariate Data*, edited by V. Barnett, pp. 21–36, John Wiley, Chichester.
- Tomasella, J., M. G. Hodnett, L. A. Cuartas, A. D. Nobre, M. J. Waterloo, and S. M. Oliveira (2008), The water balance of an Amazonian micro-catchment: The effect of interannual variability of rainfall on hydrological behaviour, *Hydrol. Process.*, 22(13), 2133–2147.
- Tomasella, J., L. S. Borma, J. A. Marengo, D. A. Rodriguez, L. A. Cuartas, A. C. Nobre, and M. C. R. Prado (2011), The droughts of 1996–1997 and 2004–2005 in Amazonia: Hydrological response in the river main-stem, *Hydrol. Process.*, 25(8), 1228–1242.
- Vourlitis, G. L., J. de Souza Nogueira, F. de Almeida Lobo, K. M. Sendall, S. R. de Paulo, C. A. Antunes Dias, O. B. Pinto Jr., and N. L. R. de Andrade (2008), Energy balance and canopy conductance of a tropical semi-deciduous forest of the southern Amazon Basin, *Water Resour. Res.*, 44, W03412, doi:10.1029/2006WR005526.
- Zeng N., J. H. Yoon, J. A. Marengo, A. Subramaniam, C. A. Nobre, A. Mariotti, and J. D. Neelin (2008), Causes and impacts of the 2005 Amazon drought. *Environ. Res. Lett.*, 3(1), 014002, doi:10.1088/1748-9326/3/1/014002.